



Bioreactivity of dissolved organic carbon in ponds of the ice-wedge polygonal tundra

Thomas Pacoureau^{1,2,3}, Milla Rautio^{2,3,4}, Isabelle Laurion^{1,2,3}

- ¹Laboratoire de limnologie nordique, Centre Eau Terre Environnement, Institut national de la recherche scientifique, Québec, QC, G1K 9A9, Canada
- ²Centre for northern studies, Université Laval, Québec, QC, G1V 0A6, Canada
- ³Interuniversity research group in limnology, Université de Montréal, Montréal, QC, H3C 3J7, Canada
- ⁴Laboratoire des sciences aquatiques, Département des sciences fondamentales, Université du Québec à Chicoutimi, Chicoutimi, QC, G7H 281, Canada
- 10 Correspondence to: Thomas Pacoureau (thomas.pacoureau@gmail.com)

Abstract. The role of ponds in transforming laterally exported dissolved organic matter (DOM) within polygonal landscapes affected by degrading ice-wedges remains poorly understood, despite their potential importance in carbon cycling. We hypothesized that the morphological and limnological diversity of ponds-driven by permafrost erosion and soil subsidencegenerates DOM of varying bioreactivity. To test this, we conducted a 188-day bioassay using water from 15 ponds representing the main geomorphological pond types in a polygonal landscape in northeastern Canada. Using optical spectroscopy, we examined the relationship between DOM properties and its bioreactivity. We also conducted a parallel bioassay experiment with nutrient additions to assess potential inorganic nitrogen and phosphorus limitations. Results show that a significant proportion of dissolved organic carbon (DOC) is available to bacterioplankton in these shallow lentic systems during summer (33% decomposed after 97 days). Contrary to our hypothesis, and despite variations in DOM composition, no difference in DOC loss was observed among the three pond categories defined in this study, suggesting comparable bioavailable DOC pools. Moreover, nutrient addition did not significatively enhance DOC loss or decay rates, suggesting that bacterial decomposition depends mainly on organic matter bioavailability. This is further supported by a positive correlation between DOC loss and tryptophan-like fluorophores, a marker of bioavailable DOM. This suggests that DOM released by cyanobacterial mats and other autochthonous producers may be more readily utilized by bacteria than DOM derived from peaty soils. These findings highlight the importance of freshly produced organic matter in regulating carbon cycling in ponds of the ice-wedge polygonal tundra, with consequences on the fate of carbon released from thawing soils.

1 Introduction

Accelerated warming in the Arctic is driving the thaw and erosion of ice-rich permafrost, mobilizing vast reservoirs of previously frozen organic carbon (Liljedahl et al., 2016; Olefeldt et al., 2016; Nitze et al., 2018). A significant portion of this carbon is transported to inland waters as dissolved organic matter (DOM) (Abbott et al., 2015; Vonk et al., 2015a; Zhang et al., 2017), with tundra ponds–comprising up to 95% of water bodies in some regions (Muster et al., 2013)–acting as primary





recipients. While small permafrost ponds (< 1000 m²) are recognized for their role in greenhouse gas exchange (Abnizova et al., 2012; Kuhn et al., 2018; Lougheed et al., 2020; Karlsson et al., 2021; Prėskienis et al., 2021), their capacity to transform DOM from thawing soils and growing vegetation remains understudied.

In ice-wedge polygonal tundra, permafrost erosion releases potentially highly biodegradable DOM (Vonk et al., 2019). The source and chemical composition of DOM likely determine its bioreactivity (Abbott et al., 2014), but linking bioreactivity to specific DOM fractions is challenging due to its chemical complexity and diverse, seasonally shifting sources. In permafrost regions, these sources include organic compounds leached from thawing permafrost and its surface active layer, as well as compounds produced by aquatic plants, benthic or planktonic algae, and bacterioplankton (Wauthy et al., 2018; Ma et al., 2019). Absorption and fluorescence spectroscopy are valuable tools for characterizing DOM's functional properties (Ateia et al., 2017; Stubbins et al., 2014; McCallister et al., 2018), but the relationship between 'colored' (CDOM) and fluorescent (FDOM) DOM fractions and their bioreactivity remains poorly understood (Guillemette and del Giorgio, 2012; Lapierre et al., 2013; Berggren et al., 2020). In Canada's organic, syngenetic permafrost deposits, Fouché et al. (2020) highlighted the release of potentially bioavailable FDOM due to active layer thickening and permafrost erosion, while cyanobacterial mats, mosses, and aquatic plants have also been identified as significant sources of bioavailable FDOM in thaw ponds on similar deposits (Pacoureau et al., 2025). Understanding the fate of DOM entering thaw ponds and the biogeochemical drivers of its bioreactivity is essential for refining regional carbon budgets and predicting Arctic watershed response to climate warming. Alongside potentially bioavailable DOM, permafrost thaw leads to increased inorganic nitrogen (N) and phosphorus (P) in surface waters (Vonk et al., 2015a; Fouché et al., 2020; Tank et al., 2020; Pacoureau et al., 2025). Enhanced N and Pavailability 50 can stimulate bacterial growth and increase dissolved organic carbon (DOC) turnover rates (Mann et al., 2014; Allesson et al., 2020; Berggren et al., 2023). These macronutrients, especially P, have been shown to regulate bacterioplankton growth in temperate and boreal surface waters, often in conjunction with organic carbon (Smith and Prairie, 2004; Berggren et al., 2010; Vidal et al., 2011). This pattern of P-limitation appears consistent across oligotrophic lakes in subarctic and Arctic regions (Granéli et al., 2004; Rodríguez et al., 2013). However, the extent to which nutrients influence DOC decomposition in high-DOM thaw ponds remains uncertain. In nutrient-poor permafrost thaw streams, adding inorganic N and P to achieve nutrientreplete conditions has been shown to double DOC turnover (Textor et al., 2019). Similar additions to waters from thermokarst features-varying in ambient DOC and nutrient levels-nearly doubled the amount of rapidly decomposed DOC (i.e., DOC lost within 10 days) but had no effect on total DOC degraded over 40 days (Abbott et al., 2014). The role of nutrient availability in bacterial DOC decomposition likely varies across the heterogeneous ponds of polygonal tundra, which differ widely in morphology, thermokarst erosion, plant colonization, and transparency, factors influencing bacterial exposure to bioreactive carbon and nutrients (Pacoureau et al., 2025; Preskienis et al., 2024, 2021). Experimental studies are therefore needed to predict how thawing permafrost will influence bacterial DOC decomposition and mineralization. In this study, we assessed DOM bioreactivity in the water column of three representative pond types commonly found in

landscapes with degrading ice-wedge polygons underlain by organic-rich syngenetic permafrost. These included: (1) eroding ice-wedge trough (eIWT) ponds, which receive DOM inputs from surrounding soils and active permafrost thaw; (2) stable ice-





wedge trough (sIWT) ponds, which show no signs of permafrost erosion and are colonized by vegetation; and (3) coalescent polygon (CP) ponds, characterized by clearer waters and lower hydrological connectivity to the surrounding terrestrial environment. We incubated water samples for 188 days under dark, oxygenated conditions, with replicates amended with inorganic N and P to simulate nutrient-replete conditions. We hypothesized that: (i) eIWT ponds would experience greater DOC loss than stable aquatic features (sIWT and CP ponds), due to higher inputs of bioavailable DOC from permafrost erosion and surrounding soils; and (ii) nutrient addition would not increase DOC turnover rates across all pond types, since these systems typically receive elevated N and P inputs relative to bioavailable allochthonous organic carbon, based on previous findings (Pacoureau et al., 2025). This study aims to provide empirical evidence about how permafrost thaw ponds process DOM, thereby improving predictions of carbon cycling and biogeochemical responses in rapidly changing Arctic landscapes.

75 2 Materials and methods

80

2.1 Study site and ponds

Bylot Island is located in the eastern Canadian Arctic, within the boundaries of Sirmilik National Park (73°09'N, 79°58'W). The study site lies in the Qarlikturvik Valley (~20 km²) on the western plain of the island. The valley features numerous lakes and ponds, surrounded by patches of both dry and wet tundra. Low- and high-centered polygons occur in organic-rich Holocene peaty-loess deposits (1.6–27% OC in the upper meter; Prėskienis, 2022) with excess pore ice. Collectively, these soils store an estimated 1,654 Tg C in the top meter, with an average OC stock of 82 kg C m⁻² (Ola et al., 2022). In this type of deposits, the thickness of the active layer typically varies from 30 to 70 cm (Allard et al., 2024). Climatic data for the period 1994–2019 indicate an average annual temperature of -14.4°C, with only 78 mm of precipitation on average between June and August (CEN, 2020).

Ponds ranging in surface area from 26 to 997 m² (median: 178 m²) were selected to capture the geomorphological and limnological variability characteristic of ice-wedge polygonal landscapes. Using the classification formerly employed by Pacoureau et al. (2025), we sampled five ponds from each of the following categories: (i) eroding ice-wedge trough (eIWT) ponds, (ii) stable ice-wedge trough (sIWT) ponds, and (iii) coalescent polygon (CP) ponds. In brief, eIWT ponds are elongated, water-filled troughs that form above melting ice wedges surrounding high-centered polygons. As these ponds gradually accumulate sediments and organic matter and undergo vegetation encroachment, ice-wedge degradation slows, leading to the transition of eIWT ponds into sIWT ponds. CP ponds, on the other hand, develop from soil subsidence in polygonal terrain, resulting from the merging of multiple ponds. They are characterized by transparent waters and thick benthic cyanobacterial mats. All studied ponds are very shallow (< 1.5 m) and freeze completely to the bottom from late September to mid-June.

2.2 Sampling

A total of 15 ponds were sampled on July 27, 2017. In situ temperature and dissolved oxygen were measured with a YSI multiparameter probe (Yellow Springs, OH, USA). Subsequently, two liters of water were collected from ~20 cm below the





surface at the deepest point of each pond, using a peristaltic pump attached to a laminar sampler (for more details, see Fig. S3 in Matveev et al., 2019). Samples were stored in polycarbonate bottles and placed in a cooler until processing at the field station within 2.5 hours.

100 **2.3 Bioassay**

110

115

120

Samples were filtered through pre-combusted grade D glass fiber filters (2.7 µm nominal retention, Whatman) to eliminate the need for an inoculation step and to exclude crustacean grazers and most nanoflagellate bacterivores. While bioassay sample preparation often involves filtration through membranes with nominal retention between 0.7 and 0.2 µm, these smaller pore sizes tend to retain a greater number of bacterial cells (Dean et al., 2018), particularly those attached to small particles, which are abundant in thaw ponds and account for over 50% of the total bacterial population and biomass production (Breton et al., 2009; Roiha et al., 2015; Deshpande et al., 2016). Additionally, using smaller filter cut-off to remove bacterivores may disrupt the microbial loop that drives nutrient remineralization during extended incubations. Therefore, using a larger pore size filter likely produces DOC degradation dynamics that more closely reflect in situ conditions.

Samples were incubated in 1-liter polycarbonate bottles, with an air headspace occupying 20% of the total volume. Incubation units were kept in the dark to reflect heterotrophic microbial degradation and maintained at a constant temperature of 15° C. Although this is approximately 5° C higher than the average surface water temperature at the time of sampling (daytime mean $\pm 1\sigma$ at 20 cm depth = $10.1 \pm 1^{\circ}$ C), 15° C was chosen to ensure standardized experimental conditions rather than to replicate in situ temperatures. This temperature was preferred over the more commonly used 20° C to minimize the risk of overestimating DOC loss, and because it is a standard choice in bioassays involving Arctic waters (Vonk et al., 2015b; Wyatt and Rober, 2020).

To assess the potential effect of nutrient limitation on bacterial DOM decomposition, replicate incubation units were amended with sodium nitrate (NaNO₃), ammonium chloride (NH₄Cl), and monopotassium phosphate (KH₂PO₄) to increase ambient NO₃-NH₄+ and PO₄³- concentrations by 80 and 10 μM, respectively, following the recommendations of Vonk et al. (2015b). Incubation units were loosely capped and gently agitated every two days. At the start of the incubation and on days 8, 15, 29, 71, 97 and 188, aliquots were collected for DOC, DOM absorbance and fluorescence measurements, and flow cytometry. Additional aliquots for total phosphorus (TP), total nitrogen (TN), and chlorophyll *a* (Chl*a*; used as a proxy for algal biomass) analyses were collected in unfiltered water prior to the start of incubation. Upon completion of the bioassay, the remaining water volume in the bottles exceeded half of the initial volume.

2.4 DOC reactivity

DOC loss was expressed both as the reduction in concentration (mg L-1) and as a percentage of the initial DOC concentration, measured at days 29, 97, and 188 of the incubation. These time points include the typical duration of bioassays (one month) as well as extended incubation periods. Aliquots for DOC analysis were filtered through pre-combusted grade F glass fiber filters (0.3 µm nominal retention, Advantec) and stored at 4°C in pre-combusted amber borosilicate glass vials, following



135

140

145

150

160



acidification with sulphuric acid to a pH of approximately 2. DOC concentrations were determined using an Aurora 1030W TOC analyser (OI Analytical, College Station, TX, USA) following persulfate digestion (EPA Method 415.1). Blanks were prepared on each sampling day by filtering ultrapure water (Milli-Q®), and all DOC concentrations measured were below the detection limit of 0.1 mg C L⁻¹.

To describe DOC decomposition dynamics, we compared four commonly used models: a linear model, an exponential decay model, an exponential decay model with a residual DOC pool, and the gamma reactivity continuum model (as in e.g. Koehler et al., 2012). Models were fitted to the relative DOC loss over time (DOC $_t$ /DOC $_0$) for each incubation unit using R Statistical Software v4.3.3 (R Core Team, 2024). Linear models were applied using the 'lm' function, while nonlinear models were fitted using the 'nls' function, both from the built-in *stats* package.

Model selection was based on the sum of Akaike weights and the root mean square error (RMSE) calculated for each DOC decomposition time course. Akaike weights, derived from the corrected Akaike Information Criterion (AICc), reflect the probability of each model being the best among the set. RMSE was used to assess goodness-of-fit, with lower values indicating better model performance. It is important to note that the parameters estimated by each model differ according to their underlying assumptions. Both the linear and exponential decay models provide decay rate estimates (k, day⁻¹), while the exponential decay model with a residual pool also estimates the fraction of DOC that is not degraded. In contrast, the reactivity continuum model yields two parameters: a (days), representing the average lifetime of the more reactive compounds, and v (dimensionless), reflecting the relative abundance of more recalcitrant compounds. A two-pool exponential decay model was also considered, but it could not be fitted due to convergence issues.

The exponential decay model with a residual pool provided the best representation of DOC decomposition during the bioassays, offering the optimal balance between Akaike weights and RMSE (see Supplementary **Table S1**). However, since the plateau at the end of the decay curve is not supported by datapoints beyond 188 days, the estimated size of the residual DOC pool may be biased (e.g., **Fig. S1**). As a result, we focused our analysis on the decay rate (k), rather than on the residual fraction. The distribution of decay rates obtained from the exponential model with residual pool closely matched the distribution of initial apparent decay rates from the reactivity continuum model (calculated as v/a, in day⁻¹). In contrast, the decay rates derived from the simple exponential model were similar to those from the linear model, which showed the poorest performance among the models tested (**Fig. S2**).

155 2.5 DOM optical analysis

Samples for DOM optical analysis were filtered through pre-combusted grade F glass fiber filters, and stored at 4°C without headspace or any preservative. UV-Vis absorbance spectroscopic analyses were performed on a dual-beam Cary 100 UV-Vis spectrometer (Agilent, Santa Clara, USA), with ultrapure water serving as the blank. Scans were collected at room temperature from 200 to 800 nm in 1 nm increments, and spectra were baseline-corrected by subtracting the mean absorbance between 790 and 800 nm. Napierian absorption coefficients were calculated by multiplying absorbance by 2.303 and dividing by the pathlength of the quartz cuvette (0.01 m). The absorption coefficient at 320 nm (a₃₂₀, in m⁻¹) was used as a proxy for the





concentration of CDOM, the specific ultraviolet absorbance at 254 nm (SUVA₂₅₄, in L mg C⁻¹ m⁻¹) served as an indicator of DOM aromaticity (Weishaar et al., 2003), and the spectral slope coefficient between 275 and 295 nm (S₂₈₅, in nm⁻¹) was used as a proxy of DOM molecular weight (Helms et al., 2008).

165 To further characterize DOM at the start of the bioassay, fluorescent excitation-emission matrices (EEMs) were generated using a Cary Eclipse spectrofluorometer (Agilent, Santa Clara, CA, USA). Excitation wavelengths ranged from 240 to 450 nm in 5 nm increments, and emission wavelengths ranged from 300 to 560 nm in 2 nm increments. EEMs were corrected following the methodology of Murphy et al. (2013) using the FDOMcorr toolbox v1.6, and analyzed, along with other samples from the study site, using parallel factor analysis (PARAFAC). For details on the samples used for PARAFAC modelling and the procedure, refer to Pacoureau et al. (2025). The analysis identified four humic-like fluorescence components classified as 'terrestrial' (HT1–4) based on comparisons with reference spectra in the OpenFluor repository (www.openfluor.org, R. Murphy et al., 2014), along with two humic-like fluorescent components of 'microbial' origin (HM1–2) and two protein-like components (P1–2). The concentration of each fluorescent component (*Ci*) in a given sample was expressed as its maximum intensity (*F*_{max}) in Raman units (RU), while total fluorescence (*F*_{tot}) was calculated as the sum of all *Ci*.

175 **2.6** Nutrient and chlorophyll *a* analyses

TN and TP were determined in unfiltered samples using colorimetric methods. TN was measured on a QuickChem 8000 automated ion analyzer (Lachat Instruments, Milwaukee, WI, USA) following sample digestion (EPA Method 353.2; detection limit of 4 µg L⁻¹), and TP was measured on an Astoria 2 analyzer (Astoria-Pacific, Clackamas, OR, USA) (EPA Method 365.3; detection limits of 0.7 µg L⁻¹). Chlorophyll *a* (Chl*a*) was extracted with hot ethanol, and its concentration determined fluorometrically before and after acidification to correct for pheopigments (Nusch, 1980).

2.7 Bacterial abundance

180

185

190

Samples for bacterial counts were preserved with glutaraldehyde (1% final concentration) and stored in cryogenic vials at -80°C until analysis. Bacterial cell abundances (BA, in cell ml⁻¹) were determined using an Accuri C6+ flow cytometer (BD Biosciences, Franklin Lakes, NJ, USA). Prior to analysis, samples were thawed and sonicated in an ice bath for 5 minutes (Sonifier SFX150, Branson Ultrasonics Corporation, Brookfield, CT, USA) with pulses of 0.1 s s⁻¹ at 50% duty cycle (~10 W). This step aimed to ensure that most particle-attached bacteria were included in the cytometric counts. Aliquots were stained in the dark with 25 μl of SYBR Green I (2.5X final concentration; Invitrogen S7563) for 15 minutes. Samples were then analyzed in triplicate for 1 minute each at slow flow rate, with a green fluorescence (FL1) intensity threshold set at 700 and acquisition in log mode. If necessary, samples were diluted with distilled water to keep the count rate below 1000 events per second to prevent coincidence. The cytometer's flow rate was calibrated on each analysis day by running a BD TrucountTM Absolute Counting Tube (total volume 2 ml) in triplicate at the beginning and end of the session. All samples received 1 μm yellow-green fluorescent microspheres as a particle size standard. Manual gating was performed using BD Accuri C6+



195

200

205

210



software to discriminate bacteria from other particles using FL1 versus red fluorescence (FL3) plots, and to delineate bacterial populations using the side-scatter (SSC) versus FL1 plots.

2.8 Statistical analyses

All statistical analyses were performed in R Statistical Software version v4.3.3 (R Core Team, 2024). Differences in mean DOC, TP, TN, Chl a, BA and optical properties among pond categories at the start of the bioassay were assessed using one-way analysis of variance (ANOVA) followed by Tukey honest significant difference (Tukey HSD) tests for multiple comparisons. To assess the effects of pond category (between-subject factor) and incubation day (within-subject factor) on DOC loss at days 29, 97, and 188, we conducted a two-way mixed measures ANOVA on unamended samples using the 'anova_test' function from the *rstatix* package (v0.7.0; Kassambara, 2023). This analysis was repeated to test the effects of pond category (between-subject factor) and nutrient addition (within-subject factor) on DOC loss at the end of the bioassay (day 188). Mixed ANOVAs were followed by post-hoc pairwise t-tests with Bonferroni correction for multiple comparisons (implemented in the base *stats* package in R). Prior to conducting ANOVAs, residual diagnostic plots were visually inspected to verify the assumptions of normality and homoscedasticity. Degrees of freedom were adjusted using the Greenhous-Geisser correction to avoid inflated F-ratios when the sphericity assumption was not respected for mixed ANOVAs (i.e., Mauchly's test P < 0.05).

The exponential decay model with a residual DOC pool was fitted to all data within a nonlinear mixed-effects modeling framework, using the 'nlme' function from the nlme package (Pinheiro and Bates, 2023). This approach is well-suited for data with a hierarchical structure, such as time series of DOC decomposition with samples nested within ponds. In the model, pond category (three levels: eIWT, sIWT or CP) and nutrient addition (two levels: ambient or nutrient-replete) were treated as fixed effects, with pond included as a random effect. Differences in fixed effects were tested using ANOVA, followed by pairwise comparisons using the 'emmeans' function from the emmeans package, with *P* values adjusted using the Tukey method (Lenth, 2025).

To identify which variables measured during the initial characterization of the assayed waters best explained variations in DOC loss at days 97 and 188, as well as DOC decay rates, we performed multiple linear regression analyses using pooled unamended samples from the 15 ponds. Potential explanatory variables included TP, TN, Chl a, a₃₂₀, SUVA₂₅₄, S₂₈₅, and the fluorescence intensity of each PARAFAC components (F_{max}). S₂₈₅, Chla, and P2 fluorescent component were log-transformed (log[x]+1 for P2) to improve normality. To avoid multicollinearity, PARAFAC components that were highly correlated with a₃₂₀ (Spearman's ρ > 0.75) were excluded from further analysis (all HT and HM components). All possible models were generated from the remaining predictors (a₃₂₀, SUVA₂₅₄, Chla, TN, TP, P1, and P2), and the best models were selected based on the AICc for small samples, retaining those within ΔAICc ≤ 5 of the top-ranked models. Models were ranked according to their Akaike weights using the 'lm' function (base *stats* package) and the 'dredge' function (MuMIn package; Bartoń, 2024). The quality of the retained models was assessed using diagnostic plots and examination of residual heteroscedasticity.





225 3 Results

230

235

240

245

3.1 Initial characterization of the assayed waters

We detected differences in DOC and TP concentrations among pond categories at the onset of the bioassay (**Table 1**). Mean DOC and TP concentrations in eIWT ponds were 1.3 and 1.6 times higher, respectively, compared to concentrations in CP ponds. In contrast, mean concentrations of TN and Chla did not differ among pond categories. Although bacterial abundance showed slight variations among pond categories, mean values remained within the same order of magnitude. DOM was more colored in eIWT ponds, with CDOM (expressed as a_{320}) decreasing twofold and fourfold in sIWT and CP ponds, respectively. SUVA₂₅₄ indicated decreasing proportion of aromatic structures from eIWT to CP ponds, with sIWT ponds having intermediate values, and the slope S₂₈₅ a lower apparent molecular weight in CP ponds compared to ice-wedge trough ponds. DOM was more fluorescent in eIWT ponds, with FDOM (expressed as F_{tot}) being 1.7 and 2.4 times higher than those in sIWT and CP ponds, respectively. PARAFAC analysis revealed the dominance of terrestrial humic-like components in the ponds (**Fig. 1**), particularly component HT1. All HT components decreased between eIWT and sIWT or CP ponds (for HT2, eIWT > sIWT > CP). Microbial humic-like components also varied among pond categories, with higher mean fluorescence in eIWT ponds compared to sIWT and CP ponds. The tryptophan-like component (P1) generally dominated the total amino acid-like fluorescence in our dataset (range 0.25–0.58 RU). P1 and the tyrosine-like component (P2) did not showed differences in mean fluorescence among pond categories.

Table 1: Initial characterization of the assayed waters. Ranges are presented for each parameter, with mean \pm SE (n = 5) for each pond category. Mesological conditions include dissolved organic carbon (DOC), total phosphorus (TP), total nitrogen (TN), chlorophyll a as a proxy for phytoplankton biomass, bacterial abundance (BA), dissolved organic matter (DOM) absorption coefficient at 320 nm (a₃₂₀), specific ultraviolet absorbance at 254 nm (SUVA₂₅₄), spectral slope estimated between 275 and 295 nm (S₂₈₅), and total fluorescence intensity (F_{tot}). Within each row, different letters represent significant differences between pond categories according to Tukey's HSD test (P < 0.05).

	Range	Eroding ice-wedge troughs (eIWT) ponds	Stabilized ice- wedge troughs (sIWT) ponds	Coalescent polygon (CP) ponds	One-way ANOVA, F _(2, 12)
DOC and nutrients					
DOC (mg L ⁻¹)	10.6-18.5	17.4 ± 0.24 ^a	14.8 ± 1.14 ^{ab}	13.3 ± 1.23 ^b	$F = 4.43, P = 0.036, \eta^2 = 0.42$
TP (μg L ⁻¹)	16.0-52.1	43.3 ± 1.89 ^a	28.6 ± 6.15^{ab}	25.8 ± 3.01b	$F = 5.29$, $P = 0.023$, $\eta^2 = 0.47$
TN (μg L ⁻¹)	753-1198	1010 ± 31	924 ± 75	1003 ± 75	$F = 0.56$, $P = 0.58$, $\eta^2 = 0.09$
Biological parameters					
Chl <i>a</i> (μg L ⁻¹)	0.3-12.6	2.35 ± 0.65	1.92 ± 0.98	4.57 ± 2.28	$F = 0.92, P = 0.42, \eta^2 = 0.13$
BA (x 10 ⁶ cell ml ⁻¹)	0.9-4.4	2.56 ± 0.67	1.08 ± 0.08	1.68 ± 0.22	$F = 3.29$, $P = 0.073$, $\eta^2 = 0.35$
DOM optical properties					
a ₃₂₀ (m ⁻¹)	11.3-74.0	60.8 ± 3.91ª	33.0 ± 5.92b	14.8 ± 7.24 ^c	$F = 26.44$, $P = 4.01 \times 10^{-5}$, $\eta^2 = 0.82$
SUVA ₂₅₄ (L mg C ⁻¹ m ⁻¹)	1.3-3.2	3.40 ± 0.12^{a}	2.42 ± 0.26^{a}	1.53 ± 0.13b	$F = 5.37$, $P = 0.022$, $\eta^2 = 0.47$
S ₂₈₅ (nm ⁻¹)	0.012-0.024	0.013 ± 0^{a}	0.016 ± 0.001^{a}	0.021 ± 0.001b	$F = 19.77$, $P = 1.59 \times 10^{-4}$, $\eta^2 = 0.7$
F _{tot} (RU)	1.7-6.3	5.77 ± 0.228 ^a	3.42 ± 0.366b	2.44 ± 0.472b	$F = 21.51$, $P = 1.08 \times 10^{-4}$, $\eta^2 = 0.78$





3.2 DOC loss

260

At ambient nutrient concentration, DOC loss ranged between 0.3–7.1 mg L⁻¹ (2–41% of initial DOC) across all samples and incubation times. No difference was detected in mean DOC loss among pond categories for absolute concentrations (mixed ANOVA: $F_{(2, 12)} = 0.18$, P = 0.84, η^2 G = 0.02) or relative concentrations ($F_{(2, 12)} = 1.82$, P = 0.2, η^2 G = 0.17) (**Table S2**). However, DOC loss varied along the incubation both for absolute ($F_{(1.19, 14.32)} = 126.75$, $P = 7.53 \times 10^{-9}$, η^2 G = 0.82) and relative concentrations ($F_{(1.39, 16.71)} = 289.79$, $P = 8.02 \times 10^{-13}$, η^2 G = 0.88) (**Fig. 2**). Mean DOC loss increased between day 29 (mean \pm SE: 1.0 ± 0.3 mg L⁻¹ or $7.1 \pm 1.7\%$) and day 97 (5.0 ± 0.2 mg L⁻¹ or $33.2 \pm 1.1\%$), plateauing from day 97 until the end of the assay at day 188 (5.0 ± 0.3 mg L⁻¹ or $33.4 \pm 1.2\%$).

For nutrient-replete incubations, DOC loss ranged between 0.1-8.5 mg L⁻¹ (1–46% of initial DOC) across all samples and incubation times. DOC loss was not affected by nutrient addition, either in terms of absolute (mixed ANOVA: $F_{(2,12)}=0.1$, P=0.76, η^2 G = 0.002) or relative concentrations ($F_{(2,12)}=0.183$, P=0.68, η^2 G = 0.007) (**Table S2**). There was no detectable effect of the interaction between pond category and nutrient addition on absolute ($F_{(2,12)}=1.724$, P=0.22, η^2 G = 0.06) and relative DOC loss ($F_{(2,12)}=1.627$, P=0.237, η^2 G = 0.11).

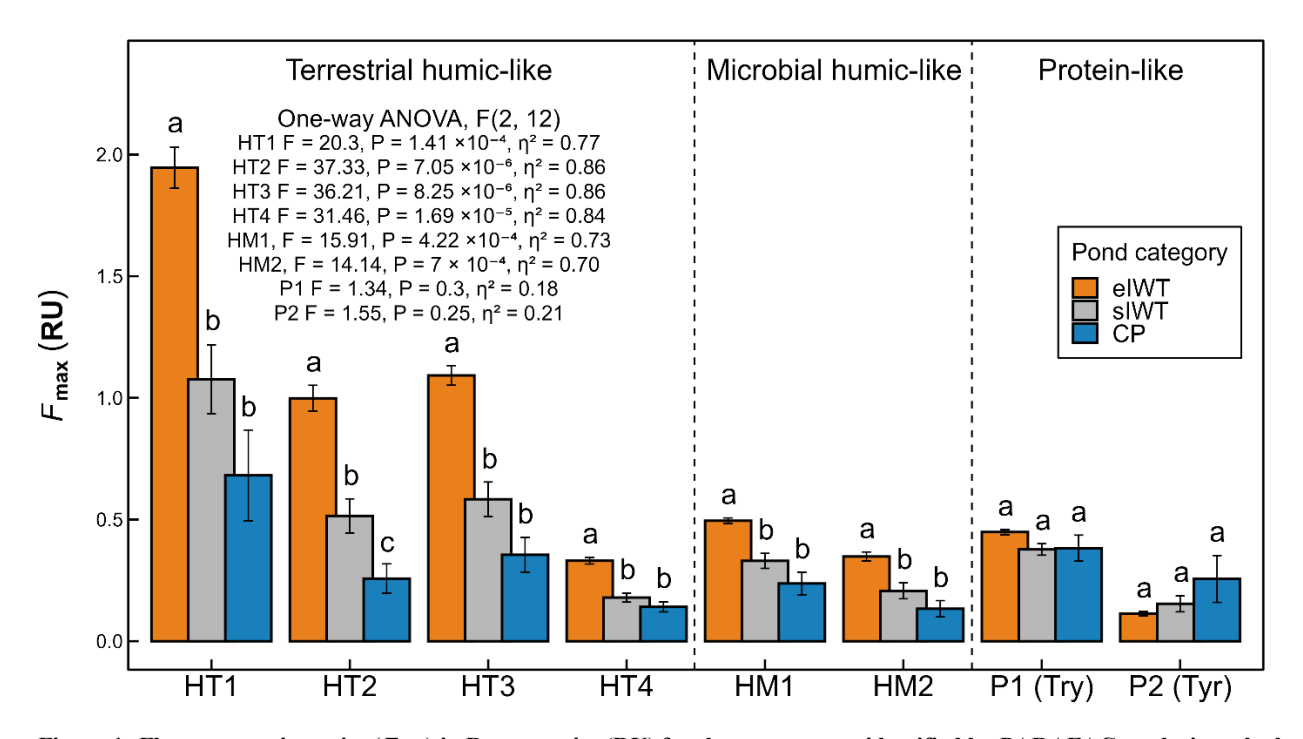


Figure 1: Fluorescence intensity (F_{max}) in Raman units (RU) for the components identified by PARAFAC analysis at the beginning of the bioassay (mean \pm SE, n = 5). The components are divided to terrestrial humic-like (HT1-HT4), microbial humic-like (HM1 and HM2), and protein-like (tryptophan-like component P1 = Try, and tyrosine-like component P2 = Tyr) according to their fluorescence characteristics. P values are adjusted using the Tukey method. For each component, different letters represent significant differences between pond categories as determined by Tukey HSD tests (P < 0.05).





270

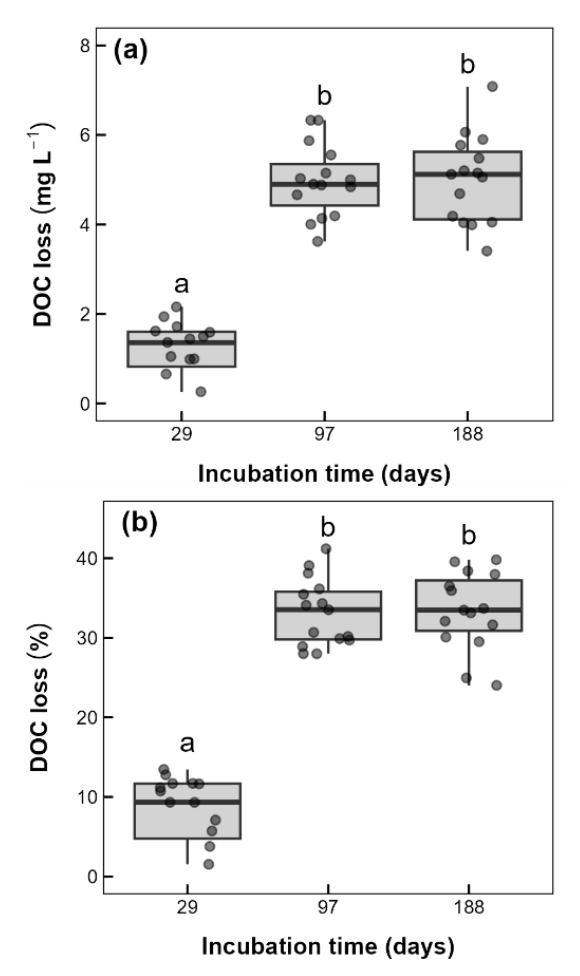


Figure 2: DOC loss during the 188-day dark bioassay using 2.7 μ m-filtered pond water incubated at 15°C. Results are expressed as DOC loss (a) and percentage DOC loss relative to initial DOC concentration (b). Boxplots indicate median (line), 1st and 3rd quartile (box margins), and 5 and 95% percentiles (whiskers). Different letters represent significant differences as determined by pairwise t-tests with Bonferroni correction (P < 0.0001).

3.3 DOC decay rates

275

280

Decay rates (k) ranged from 0.009 to 0.034 day⁻¹ in unamended samples and from 0.011 to 0.063 day⁻¹ in nutrient-replete samples (**Fig. 3**). Both pond category (F-tests for fixed effects: $F_{(2,181)} = 20.1$, $P = 1.35 \times 10^{-8}$) and nutrient addition ($F_{(1,181)} = 32.8$, $P = 4.25 \times 10^{-8}$) had significant effects on k. The interaction between the two factors indicated that the effect of nutrient addition on k depended on pond category ($F_{(2,181)} = 137.1$, $P = 6.14 \times 10^{-24}$). However, pairwise comparisons did not reveal any differences among group means; the lowest P-value observed was 0.31 for the comparison between unamended eIWT and CP ponds (**Fig. 4**). Notably, the estimated means were associated with considerable uncertainty.





3.4 Drivers of DOC bioreactivity

Regression analysis revealed that the fluorescence intensity of the tryptophan-like component P1 was the strongest predictor of DOC loss on days 97 and 188 of the bioassay (Fig. 5). Models using P1 intensity as the sole predictor had substantially higher Akaike weights—0.42 and 0.41 for days 97 and 188, respectively—compared to the next best models, which had weights of 0.19 and 0.14 for the same time points. The decline in P1 fluorescence over time was also evident in EEMs collected at the beginning and end of the bioassay (Fig. 6). This result was consistent with the temporal dynamics of the individual PARAFAC components, showing a steady decrease in P1 fluorescence throughout the experiment (Fig. S3). In addition, regression analysis indicated that higher levels of CDOM were associated with lower decay rates (Fig. 5).

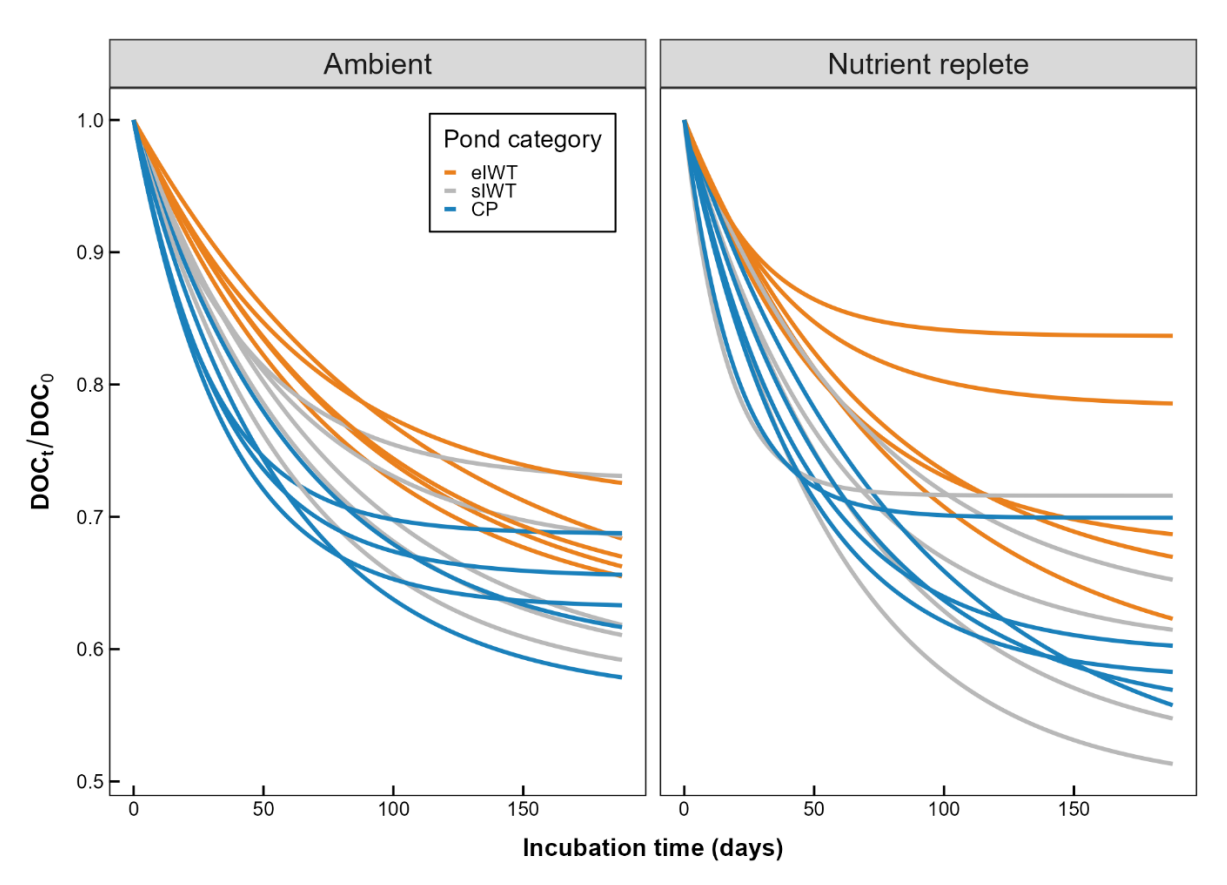


Figure 3: Exponential decay model with residual DOC pool fitted to the time series of relative DOC decomposition during the 188-day dark bioassay using 2.7 µm-filtered pond water incubated at 15°C. The samples were incubated at ambient nutrient concentrations or amended with inorganic nitrogen and phosphorus (nutrient replete).





4 Discussion

300

305

310

315

4.1 Extended microbial DOC decomposition in ice-wedge polygonal tundra ponds exceeds short-term estimates

Our results demonstrate substantial DOC decomposition by heterotrophic bacteria in the sampled ponds during the growing season, occurring on a timescale that exceed that of traditional bioassays. Most of the bioreactive DOC was processed after one month, with DOC losses exceeding 30% (or 5 mg L⁻¹) by day 97 of the bioassay, after which no further losses were observed (**Fig. 2**). DOC bioavailability is typically assessed using standardized bioassays that measure DOC disappearance or CO₂ production over a period of days to weeks (McDowell et al., 2006; Vonk et al., 2015b). However, this timeframe is likely much shorter than the actual water residence time in the hydrologically isolated ponds of the polygonal tundra. Hence, short-term bioassays may substantially underestimate microbial DOC decomposition in Arctic ponds charac terized by limited summer runoff. In this regard, our findings are consistent with those of Vähätalo and Wetzel (2008), who showed that wetland-derived organic carbon can be degraded in surface waters given a sufficiently long residence time. They also reinforce the relevance of the concept of 'hydrological biolability', introduced by Vonk et al. (2013), which emphasizes that the degradability of organic matter must be considered within the context of a system's water residence time. While short-term incubations (e.g., one month) remain useful for comparing DOM biolability across seasons or systems, they are likely to underestimate carbon loss when they do not reflect the duration of organic matter retention in aquatic environments.

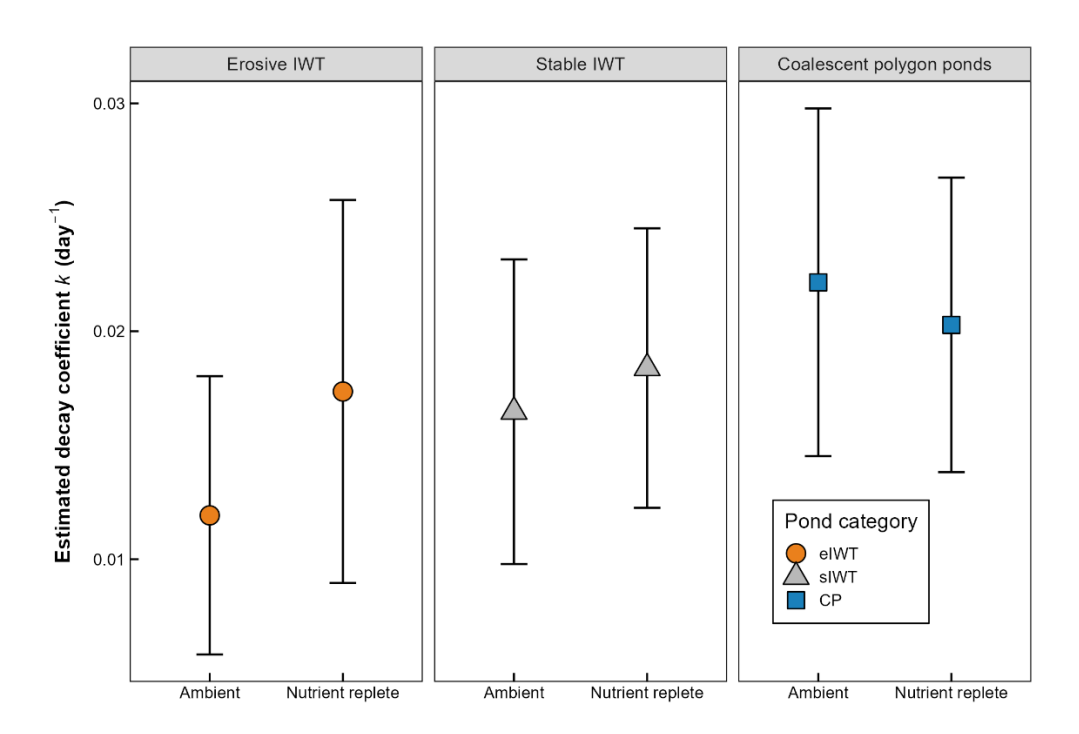


Figure 4: Estimated mean DOC decay coefficients and their 95% confidence intervals among the three water body types for ambient nutrient concentrations compared to nutrient replete treatment.



320

325

330

335

340

345



DOC loss measured during the first month of incubation $(1.0\pm0.2~\text{mg}\,\text{L}^{-1}~\text{or}\,7.1\pm1.7\%$ by day 29) was nonetheless consistent with previous studies. Earlier field incubations conducted in ponds within the same polygonal complex reported negligible DOC loss over a 12-day period, under the combined influence of microbial decomposition and sunlight exposure (Laurion et al., 2021). In the latter study, water was collected following a particularly dry period, which likely limited the input of fresh DOM to the ponds. Our estimates over this timescale also falls within the range of bioavailable DOC reported for other aquatic systems in permafrost regions. For exemple, DOC loss in lakes, streams, and rivers across Alaska, Siberia, and western Canada has been reported to range between 3% and 18% within one month (Vonk et al., 2015b). Similarly, bioassays of comparable duration conducted in waters from frozen peat bogs in Northern Europe and a thermo-erosion gully on the Tibetan Plateau (discontinuous permafrost) yielded DOC losses ranging from 0% to 10% (Liu et al., 2018; Shirokova et al., 2019). Collectively, these results suggest that the most bioreactive compounds (i.e., those mineralized over the first weeks or so) constitute a relatively small fraction of the total DOC pool in aquatic systems influenced by organic-rich permafrost, and that ponds within the ice-wedge polygonal landscapes of the eastern Canadian Arctic conform to this broader pattern.

Although higher than previous estimations made over shorter timescales for similar environments, DOC loss measured in the

eIWT ponds of Bylot Island (mean of 33% after 188 days) was lower than values reported for thermokarst aquatic systems underlain by Pleistocene-age loess deposits, commonly referred to as Yedoma. Experimental thawing of Yedoma has shown that a large portion of its DOC pool (~50%) can be rapidly utilized by bacteria in soil pore water (Drake et al., 2015). Supporting the view of a highly labile Yedoma carbon pool, DOC availability for bacterial uptake measured within 40 days is generally higher in thaw streams and outflows (12%-62%) compared to undisturbed reference sites or main river stem (6%-17%) (Abbott et al., 2014; Mann et al., 2015; Spencer et al., 2015; Vonk et al., 2013). Although DOM bioavailability varies along the soil-water continuum and is influenced by pre-sampling conditions (e.g., rainfall) and incubation methods (Abnizova et al., 2014; Vonk et al., 2015b), these studies collectively demonstrate that DOM is generally more reactive in aquatic landscapes underlain by Yedoma than in other organic-rich permafrost settings. The high bioreactivity of Yedoma-derived DOM has been attributed to its molecular composition, notably the abundance of saturated aliphatic compounds such as lipids, proteins, and carbohydrates (Spencer et al., 2015; Textor et al., 2019). A study by MacDonald et al. (2021) comparing several permafrost-derived DOM sources in the western Canadian Arctic (including tills, diamicton, lacustrine deposits, peat, and Yedoma) found that peat and Yedoma leachates had similar proportions of aliphatic compounds and aromaticity, suggesting comparable biodegradability potentials. The lower reactivity of DOM observed in the eIWT ponds of our study may therefore reflect differences in the molecular composition of DOM leached from permafrost, influenced by the nature of the parent material—on Bylot Island, a mix of peaty soils with sand and silts—and by transformation processes occurring before freezing or after thawing (MacDonald et al., 2021; Tank et al., 2020). A more detailed characterization of DOM using ultrahighresolution mass spectrometry would provide valuable insights into its oxidation state and the relative proportions of aromatic versus aliphatic compounds in Bylot Island ponds, enabling direct comparisons with aquatic systems across regions with differing permafrost histories (Spencer et al., 2015; Textor et al., 2019; Wologo et al., 2021).







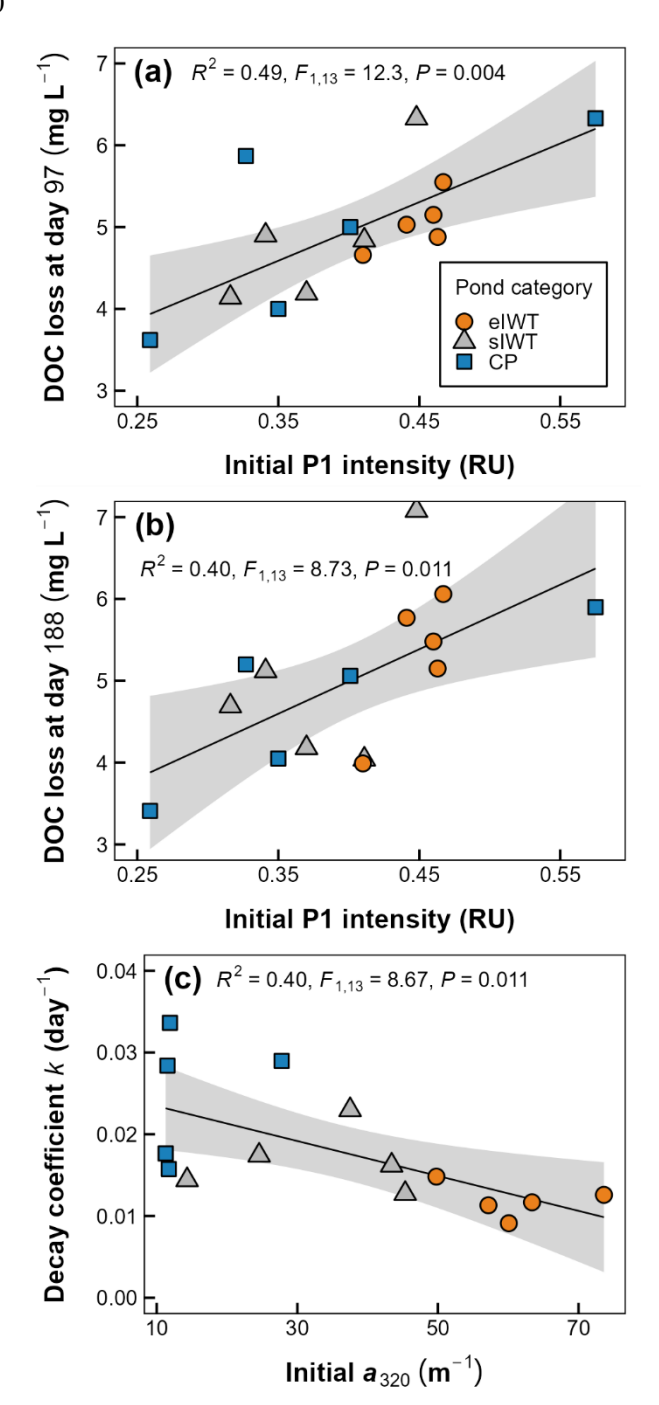


Figure 5: Relationships between the fluorescence intensity of the tryptophan-like fluorophore P1 identified by PARAFAC analysis and DOC loss at day 97 (a), DOC loss at day 188 (b), and the DOC decay rate (c).



355

360

365

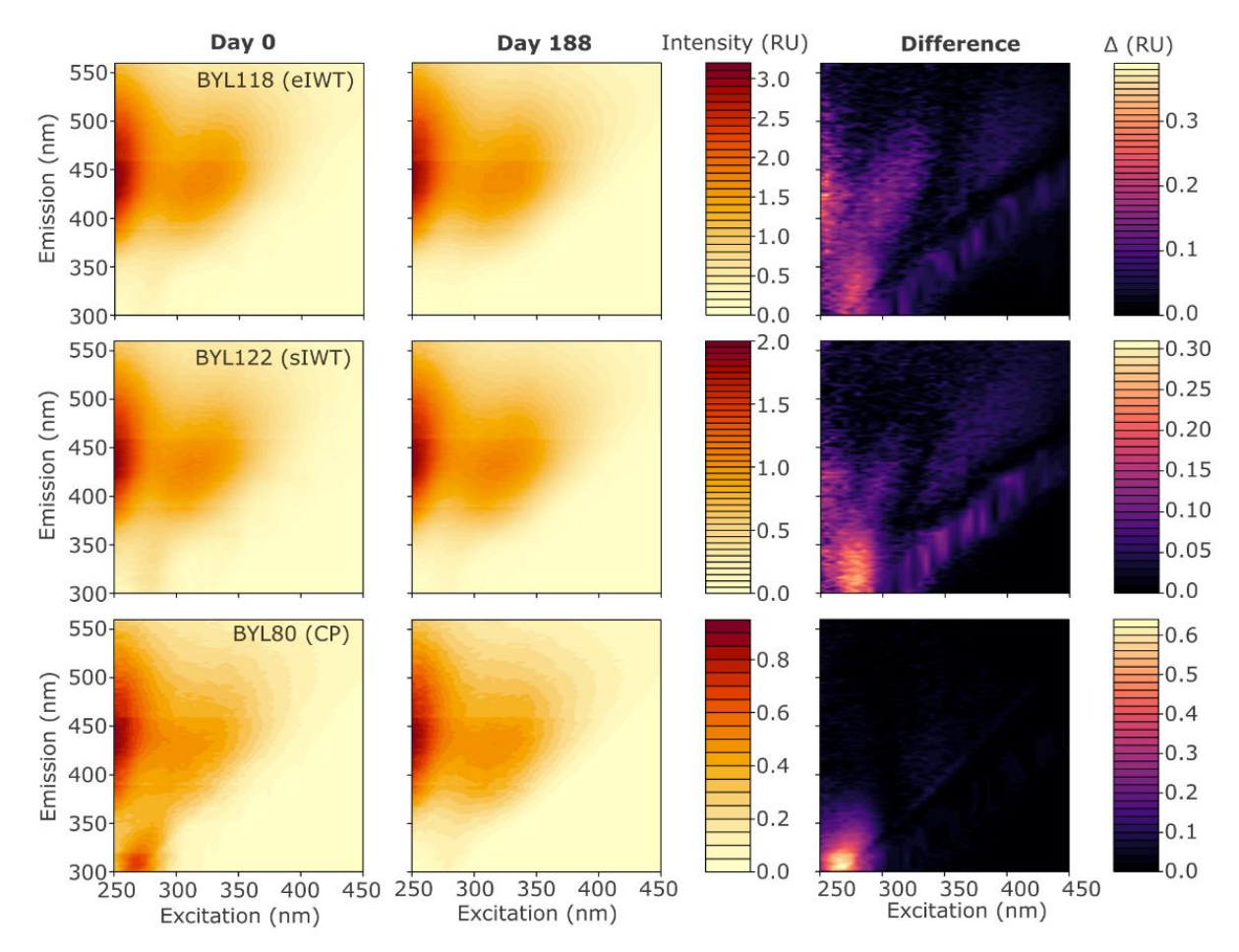


Figure 6: Representative fluorescence excitation-emission matrices (EEMs) for erosive ice-wedge trough (eIWT) ponds (top row), stable ice-wedge trough (sIWT) ponds (middle row), and coalescent polygon (CP) ponds (bottom row) at the start (left column) and end (day 188; middle column) of the bioassay. The right column shows the difference in fluorescence intensity between the two time points.

4.2 Comparable DOC loss measured despite varying levels of permafrost erosion

Contrary to our initial hypothesis, we observed comparable levels of DOC loss among the different pond categories, despite notable differences in DOC and TP concentrations and in optical properties at the start of the bioassay (**Table 1** and **Fig. 1**). This finding was unexpected, yet aligns with previous studies showing that DOM reactivity or dissolved CO₂ concentrations in surface waters are not consistently influenced by thermokarst activity (Heslop et al., 2021; Larouche et al., 2015). Two hypotheses may explain the similar DOC loss observed across ponds types in our study: (i) planktonic bacteria rely primarily on a common DOM pool across pond types, or (ii) differences in DOM composition result in similar overall losses due to



375

380

385

390

395

400



microbial community adaptation to distinct organic matter sources (Crump et al., 2003; Marschner and Kalbitz, 2003). In support of hypothesis (i), it is possible that the majority of bioavailable DOM originates from a shared external source, which is produced in situ or is modified by environmental factors such as sunlight exposure in the water column. This warrant more detailed assessments of DOM molecular composition and bacterial community structure.

4.3 No effect of nutrient addition on DOC turnover rate

Nutrient amendment in our bioassay had little to no impact on DOC loss or decomposition dynamics under the conditions tested (Figs. 3 and 4). Consistently, neither initial TP nor TN concentrations were identified as predictors of DOC loss in regression analyses. These findings suggest that the bioreactive fraction of DOC is unlikely to increase following nutrient additions in the ponds, supporting our initial hypothesis that N and P availability exceed the amount required relative to available DOC. Previous studies examining the effect of nutrient addition on DOM bioreactivity in permafrost regions have produced mixed results. For example, no effect of inorganic N and P addition was observed on BDOC in thermokarst-impacted outflows on the North slope of Alaska (Abbott et al., 2014). Conversely, negative effects on DOC mineralization were reported in streams from Canada, interior Alaska, and the Tibetan Plateau (Wologo et al., 2021), while positive effects were observed during spring freshet in Alaskan rivers (Holmes et al., 2008; Mutschlecner et al., 2018). These contrasting outcomes likely reflect variability in background nutrient availability across surface waters in permafrost regions, suggesting that carbon cycling responses to nutrient inputs are highly context-dependant. The nutrient concentrations used in our bioassay do not reflect any known scenario of nutrient enrichment in permafrost-affected surface waters, and were designed to test the potential for alleviating N and P limitation on bacterial DOC decomposition. Previous work has shown that permafrost thaw may increase N and P delivery to Arctic surface waters via runoff or drainage, as large nutrient stores become mobilized (Vonk et al., 2015a). However, in organic-rich tundra ponds such as those on Bylot Island, DOC decomposition and turnover appear largely unresponsive to nutrient enrichment. These systems already have relatively high concentrations of N and P and exhibit low C:N and C:P molar ratios (Pacoureau et al., 2025), suggesting that DOM composition-rather than nutrient availabilitymay be the primary constraint on microbial degradation.

4.4 Protein-like FDOM as an indicator of DOM bioreactivity

The positive linear relationship between the initial fluorescence intensity of the tryptophan-like component P1 and DOC loss (Fig. 5) suggests that P1 represents a significant fraction of the bioreactive DOM pool in the studied tundra ponds. This result aligns with previous research in freshwater systems and soil pore waters, where protein-like FDOM has been correlated with DOM bioreactivity and shown to be preferentially removed compared to humic-like compounds (Balcarczyk et al., 2009; Baradaran et al., 2025; Fellman et al., 2008). The similar P1 fluorescence intensities observed across pond categories (Fig. 1) may also indicate rapid cycling of these compounds in the studied systems (i.e., fast turnover rates). Although likely diverse in molecular composition, the protein-like FDOM fraction was associated with small-sized organic molecules, likely derived from aquatic and terrestrial vegetation or from cyanobacterial benthic mats (Pacoureau et al., 2025). Supporting this



405



interpretation, Allain et al. (2023) showed that leachates from vegetation collected in subarctic environments were dominated by tyrosine- and tryptophan-like fluorophores, suggesting high biolability due to the presence of lipids, amino-acids, proteins, and carbohydrates. Similarly, Textor et al. (2019) reported high microbial utilization (> 60% over 28 days) of DOC in plant leachates from the Yukon Basin in Alaska. Taken together, these findings suggest that terrestrial plants and aquatic vegetation are key precursors of biolabile DOM in tundra ponds. Their role in supporting microbial activity warrants further investigation, especially in the context of Arctic greening (Fraser et al., 2011; Ju & Masek, 2016). This trend may enhance the input of bioreactive, protein-like DOM typically associated with autochthonous production.

4.5 Fate of the remaining DOC pool

The open-water season for ponds at this latitude lasts only about 90 days (Prėskienis et al., 2021), followed by complete freezing. Given that 59%–72% of the DOC remained undegraded after ~100 days of incubation (Fig. 2), a substantial portion of this pool may ultimately form particulate organic carbon (POC) through cryoconcentration and colloid coagulation (Manasypov et al., 2015). Therefore, semi-labile and recalcitrant organic matter could accumulate in anoxic pond sediments, potentially contributing to long-term pond in filling, as previously suggested for ponds in polygonal terrains (Koch et al., 2018). Part of this POC and the remaining colloidal material may become available to bacteria during the following open-water season via re-suspension. Repeated freeze-thaw cycles have been shown to cause mechanical degradation of organic and organomineral colloids in circumneutral ponds and lakes in permafrost regions, potentially increasing DOM reactivity by generating low molecular weight compounds and removing aromatic carbon (Pokrovsky et al., 2018). Further research is needed to better understand the effect of freeze-thaw cycles on DOC dynamics in polygonal tundra ponds.

4.6 Snapshot of bacterial DOC decomposition in summer

420 Although the ice-free season is short, our study provides only a snapshot of limnological conditions and DOM decomposition potential during summer at our field site. The outcome may differ following rainfall events or during extended dry periods. Moreover, the snowmelt period, previously identified as a critical time for DOM input in tundra ponds (Fouché et al., 2017), may involve DOM of different composition and reactivity, likely altering its decomposition dynamics. Beyond microbial degradation, several processes contribute to the removal and compositional transformation of organic matter in aquatic 425 systems. These include partial or complete photo-oxidation, which breaks down organic molecules into smaller compounds or CO₂ (Wetzel et al., 1995); flocculation, which aggregates DOM into particulate form (von Wachenfeldt and Tranvik, 2008); and sorption to mineral particles (Marschner and Kalbitz, 2003). Photodegradation has received increasing attention in northern inland waters due to its role in the bleaching of CDOM and its contribution to CO₂ emissions (Bertilsson and Tranvik, 2000; Del Vecchio and Blough, 2002; Koehler et al., 2014). In addition, exposure to UV radiation has been shown to stimulate 430 microbial DOM utilization in thermokarst-impacted aquatic systems (Cory et al., 2013; Mazoyer et al., 2022). Although evidence is still lacking to fully elucidate all mechanisms involved, sunlight-induced changes in DOM composition may promote shifts in bacterial community structure and activity (Judd et al., 2007; Ward et al., 2017). In our bioassay, the high



435



contribution of chromophoric, humic-like PARAFAC components to the fluorescent DOM pool (**Fig. 1**) suggests that exposure to sunlight would likely have resulted in additional DOC losses, thereby amplifying the potential for carbon release to the atmosphere. These additional pathways (photodegradation, flocculation, and sorption to mineral particles) must be considered, as they may influence DOM fate differently than observed under dark incubation conditions such as applied in the present study.

5 Conclusion

140 landscapes over a period exceeding one month. Given the substantial DOC loss observed here, the predicted lengthening of the growing season in the Arctic, and the expanding surface area of small waterbodies characterized by permafrost thaw and erosion, microbial DOM decomposition is likely to increasingly contribute to CO₂ production in polygonal tundra ponds on Holocene peat-silt deposits. However, this contribution may remain below that of comparable waterbodies on Yedoma, due to lower DOM concentrations and bioreactivity. We showed that the protein-like FDOM fraction was linked to the concentration of bioreactive organic matter in these systems, supporting the idea that DOM composition strongly influences its lability in Arctic freshwaters. Future work should determine whether this fraction originates from modern DOM (i.e., vegetation or algal production) or from pre-aged permafrost DOM, to better assess the contribution of water column microbial processes to the permafrost carbon feedback. Finally, increased nutrient export driven by thermokarst activity may have a limited effect on DOC turnover in organic-rich thaw ponds, but this hypothesis needs to be tested across other types of permafrost aquatic systems.

Data availability

All data supporting the findings of this study are available in the Borealis repository (under review).

Author contribution

Thomas Pacoureau: conceptualization (equal), data curation (lead), formal analysis (lead), investigation (lead), methodology (lead), resources (equal), software (lead), validation (lead), visualization (lead), writing – original draft preparation (lead), writing – review & editing (equal). Isabelle Laurion: conceptualization (equal), founding acquisition (lead), investigation (supporting), methodology (supporting), project administration (lead), resources (supporting), supervision (lead), writing – review & editing (equal). Milla Rautio: conceptualization (equal), founding acquisition (supporting), writing – review & editing (equal).





460 Competing interests

The authors declare that they have no conflict of interest.

Acknowledgments

We gratefully thank F. Mazoyer for field and laboratory assistance, D. Bélanger, J. Perreault and L. Rancourt for water chemistry analysis, and F. Soulat for flux cytometry analysis. We also express our gratitude to J. Comte for providing a valuable insight on bacterial enumeration. This research was supported by the Natural sciences and engineering research council of Canada (Discovery and Northern Supplement grants to IL, and CREATE EnviroNorth scholarship to TP), and the Polar Continental Shelf Program (Natural Resources Canada). We acknowledge the Center for Northern Studies (CEN) for access to the research infrastructures, Parks Canada and the community of Mittimatalik for granting access to the study site, and the Interuniversity Research Group in Limnology (GRIL) for providing access to their analytical services. This work was carried out in the traditional territories of the Inuit, Nunangat.

References

- Abbott, B. W., Larouche, J. R., Jones Jr., J. B., Bowden, W. B., and Balser, A. W.: Elevated dissolved organic carbon biodegradability from thawing and collapsing permafrost, Journal of Geophysical Research: Biogeosciences, 119, 2049–2063, https://doi.org/10.1002/2014JG002678, 2014.
- Abbott, B. W., Jones, J. B., Godsey, S. E., Larouche, J. R., and Bowden, W. B.: Patterns and persistence of hydrologic carbon and nutrient export from collapsing upland permafrost, Biogeosciences, 12, 3725–3740, https://doi.org/10.5194/bg-12-3725-2015, 2015.
- Abnizova, A., Siemens, J., Langer, M., and Boike, J.: Small ponds with major impact: The relevance of ponds and lakes in permafrost landscapes to carbon dioxide emissions, Global Biogeochemical Cycles, 26, https://doi.org/10.1029/2011GB004237, 2012.
 - Abnizova, A., Young, K. L., and Lafrenière, M. J.: Pond hydrology and dissolved carbon dynamics at Polar Bear Pass wetland, Bathurst Island, Nunavut, Canada, Ecohydrology, 7, 73–90, https://doi.org/10.1002/eco.1323, 2014.
 - Allain, A., Alexis, M. A., Bridoux, M. C., Humbert, G., Agnan, Y., and Rouelle, M.: Fingerprinting the elemental composition and chemodiversity of vegetation leachates: consequences for dissolved organic matter dynamics in Arctic environments,
- 485 Biogeochemistry, 164, 73–98, https://doi.org/10.1007/s10533-022-00925-9, 2023.
 - Allard, M., Sarrazin, D., and l'Hérault, E.: Borehole and near-surface ground temperatures in northeastern Canada (1.6.0 (1988-2023)), https://doi.org/10.5885/45291SL-34F28A9491014AFD, 2024.
 - Allesson, L., Andersen, T., Dörsch, P., Eiler, A., Wei, J., and Hessen, D. O.: Phosphorus Availability Promotes Bacterial DOC-Mineralization, but Not Cumulative CO2-Production, Front. Microbiol., 11, https://doi.org/10.3389/fmicb.2020.569879, 2020.





- Ateia, M., Ran, J., Fujii, M., and Yoshimura, C.: The relationship between molecular composition and fluorescence properties of humic substances, Int. J. Environ. Sci. Technol., 14, 867–880, https://doi.org/10.1007/s13762-016-1214-x, 2017. Balcarczyk, K. L., Jones, J. B., Jaffé, R., and Maie, N.: Stream dissolved organic matter bioavailability and composition in watersheds underlain with discontinuous permafrost, Biogeochemistry, 94, 255–270, https://doi.org/10.1007/s10533-009-9324-x, 2009.
- Baradaran, S. C., Guillemette, F., and Lapierre, J.-F.: Abrupt shifts in the concentration, composition, and reactivity of dissolved organic carbon from terrestrial to aquatic compartments across boreal watersheds, Sci Rep, 15, 21387, https://doi.org/10.1038/s41598-025-06877-y, 2025.
 - Bartoń, K.: MuMIn: Multi-Model Inference , 2024.
 - Berggren, M., Laudon, H., Jonsson, A., and Jansson, M.: Nutrient Constraints on Metabolism Affect the Temperature
- Regulation of Aquatic Bacterial Growth Efficiency, Microb Ecol, 60, 894–902, https://doi.org/10.1007/s00248-010-9751-1, 2010.
 - Berggren, M., Gudasz, C., Guillemette, F., Hensgens, G., Ye, L., and Karlsson, J.: Systematic microbial production of optically active dissolved organic matter in subarctic lake water, Limnology and Oceanography, 65, 951–961, https://doi.org/10.1002/lno.11362, 2020.
- Berggren, M., Ye, L., Sponseller, R. A., Bergström, A.-K., Karlsson, J., Verheijen, H., and Hensgens, G.: Nutrient limitation masks the dissolved organic matter composition effects on bacterial metabolism in unproductive freshwaters, Limnology and Oceanography, 68, 2059–2069, https://doi.org/10.1002/lno.12406, 2023.
 - Bertilsson, S. and Tranvik, L. J.: Photochemical transformation of dissolved organic matter in lakes, Limnology and Oceanography, 45, 753–762, https://doi.org/10.4319/lo.2000.45.4.0753, 2000.
- Breton, J., Vallières, C., and Laurion, I.: Limnological properties of permafrost thaw ponds in northeastern Canada, Can. J. Fish. Aquat. Sci., 66, 1635–1648, https://doi.org/10.1139/F09-108, 2009.
 - CEN: Climate station data from Bylot Island in Nunavut, Canada (1.11 (1992-2019)), https://doi.org/10.5885/45039SL-EE76C1BDAADC4890, 2020.
- Cory, R. M., Crump, B. C., Dobkowski, J. A., and Kling, G. W.: Surface exposure to sunlight stimulates CO2 release from permafrost soil carbon in the Arctic, Proceedings of the National Academy of Sciences, 110, 3429–3434, https://doi.org/10.1073/pnas.1214104110, 2013.
 - Crump, B. C., Kling, G. W., Bahr, M., and Hobbie, J. E.: Bacterioplankton Community Shifts in an Arctic Lake Correlate with Seasonal Changes in Organic Matter Source, Applied and Environmental Microbiology, 69, 2253–2268, https://doi.org/10.1128/AEM.69.4.2253-2268.2003, 2003.
- Dean, J. F., van Hal, J. R., Dolman, A. J., Aerts, R., and Weedon, J. T.: Filtration artefacts in bacterial community composition can affect the outcome of dissolved organic matter biolability assays, Biogeosciences, 15, 7141–7154, https://doi.org/10.5194/bg-15-7141-2018, 2018.



535



- Del Vecchio, R. and Blough, N. V.: Photobleaching of chromophoric dissolved organic matter in natural waters: kinetics and modeling, Marine Chemistry, 78, 231–253, https://doi.org/10.1016/S0304-4203(02)00036-1, 2002.
- Deshpande, B. N., Crevecoeur, S., Matveev, A., and Vincent, W. F.: Bacterial production in subarctic peatland lakes enriched by thawing permafrost, Biogeosciences, 13, 4411–4427, https://doi.org/10.5194/bg-13-4411-2016, 2016.
 Drake, T. W., Wickland, K. P., Spencer, R. G. M., McKnight, D. M., and Striegl, R. G.: Ancient low–molecular-weight organic acids in permafrost fuel rapid carbon dioxide production upon thaw, Proceedings of the National Academy of Sciences, 112, 13946–13951, https://doi.org/10.1073/pnas.1511705112, 2015.
- Fellman, J. B., D'Amore, D. V., Hood, E., and Boone, R. D.: Fluorescence characteristics and biodegradability of dissolved organic matter in forest and wetland soils from coastal temperate watersheds in southeast Alaska, Biogeochemistry, 88, 169–184, https://doi.org/10.1007/s10533-008-9203-x, 2008.
 - Fouché, J., Lafrenière, M. J., Rutherford, K., and Lamoureux, S.: Seasonal hydrology and permafrost disturbance impacts on dissolved organic matter composition in High Arctic headwater catchments, Arctic Science, 3, 378–405, https://doi.org/10.1139/as-2016-0031, 2017.
 - Fouché, J., Christiansen, C. T., Lafrenière, M. J., Grogan, P., and Lamoureux, S. F.: Canadian permafrost stores large pools of ammonium and optically distinct dissolved organic matter, Nat Commun, 11, 4500, https://doi.org/10.1038/s41467-020-18331-w, 2020.
- Granéli, W., Bertilsson, S., and Philibert, A.: Phosphorus limitation of bacterial growth in high Arctic lakes and ponds, Aquat. Sci., 66, 430–439, https://doi.org/10.1007/s00027-004-0732-7, 2004.
 - Guillemette, F. and del Giorgio, P. A.: Simultaneous consumption and production of fluorescent dissolved organic matter by lake bacterioplankton, Environmental Microbiology, 14, 1432–1443, https://doi.org/10.1111/j.1462-2920.2012.02728.x, 2012.
- Helms, J. R., Stubbins, A., Ritchie, J. D., Minor, E. C., Kieber, D. J., and Mopper, K.: Absorption spectral slopes and slope ratios as indicators of molecular weight, source, and photobleaching of chromophoric dissolved organic matter, Limnology and Oceanography, 53, 955–969, https://doi.org/10.4319/lo.2008.53.3.0955, 2008.
 - Heslop, J. K., Hung, J. K. Y., Tong, H., Simpson, M. J., Chapman, F. M., Roulet, N., Lafrenière, M. J., and Lamoureux, S. F.: Diverging pond dissolved organic matter characteristics yield similar CO2 flux potentials in a disturbed High Arctic landscape, Environ. Res. Lett., 16, 044016, https://doi.org/10.1088/1748-9326/abc913, 2021.
- Judd, K. E., Crump, B. C., and Kling, G. W.: Bacterial responses in activity and community composition to photo-oxidation of dissolved organic matter from soil and surface waters, Aquat. Sci., 69, 96–107, https://doi.org/10.1007/s00027-006-0908-4, 2007.
 - Karlsson, J., Serikova, S., Vorobyev, S. N., Rocher-Ros, G., Denfeld, B., and Pokrovsky, O. S.: Carbon emission from Western Siberian inland waters, Nat Commun, 12, 825, https://doi.org/10.1038/s41467-021-21054-1, 2021.





- Koch, J. C., Jorgenson, M. T., Wickland, K. P., Kanevskiy, M., and Striegl, R.: Ice Wedge Degradation and Stabilization Impact Water Budgets and Nutrient Cycling in Arctic Trough Ponds, Journal of Geophysical Research: Biogeosciences, 123, 2604–2616, https://doi.org/10.1029/2018JG004528, 2018.
 - Koehler, B., von Wachenfeldt, E., Kothawala, D., and Tranvik, L. J.: Reactivity continuum of dissolved organic carbon decomposition in lake water, Journal of Geophysical Research: Biogeosciences, 117, https://doi.org/10.1029/2011JG001793,
- 560 2012.
 - Koehler, B., Landelius, T., Weyhenmeyer, G. A., Machida, N., and Tranvik, L. J.: Sunlight-induced carbon dioxide emissions from inland waters, Global Biogeochemical Cycles, 28, 696–711, https://doi.org/10.1002/2014GB004850, 2014.
 - Kuhn, M., Lundin, E. J., Giesler, R., Johansson, M., and Karlsson, J.: Emissions from thaw ponds largely offset the carbon sink of northern permafrost wetlands, Sci Rep, 8, 9535, https://doi.org/10.1038/s41598-018-27770-x, 2018.
- Lapierre, J.-F., Guillemette, F., Berggren, M., and del Giorgio, P. A.: Increases in terrestrially derived carbon stimulate organic carbon processing and CO2 emissions in boreal aquatic ecosystems, Nat Commun, 4, 2972, https://doi.org/10.1038/ncomms3972, 2013.
 - Larouche, J. R., Abbott, B. W., Bowden, W. B., and Jones, J. B.: The role of watershed characteristics, permafrost thaw, and wildfire on dissolved organic carbon biodegradability and water chemistry in Arctic headwater streams, Biogeosciences, 12,
- 570 4221–4233, https://doi.org/10.5194/bg-12-4221-2015, 2015.
 - Laurion, I., Massicotte, P., Mazoyer, F., Negandhi, K., and Mladenov, N.: Weak mineralization despite strong processing of dissolved organic matter in Eastern Arctic tundra ponds, Limnology and Oceanography, 66, S47–S63, https://doi.org/10.1002/lno.11634, 2021.
 - Lenth, R. V.: _emmeans: Estimated Marginal Means, aka Least-Squares Means_, 2025.

Environment, 627, 1276–1284, https://doi.org/10.1016/j.scitotenv.2018.01.275, 2018.

- Liljedahl, A. K., Boike, J., Daanen, R. P., Fedorov, A. N., Frost, G. V., Grosse, G., Hinzman, L. D., Iijma, Y., Jorgenson, J. C., Matveyeva, N., Necsoiu, M., Raynolds, M. K., Romanovsky, V. E., Schulla, J., Tape, K. D., Walker, D. A., Wilson, C. J., Yabuki, H., and Zona, D.: Pan-Arctic ice-wedge degradation in warming permafrost and its influence on tundra hydrology, Nature Geosci, 9, 312–318, https://doi.org/10.1038/ngeo2674, 2016.
- Liu, F., Chen, L., Zhang, B., Wang, G., Qin, S., and Yang, Y.: Ultraviolet radiation rather than inorganic nitrogen increases dissolved organic carbon biodegradability in a typical thermo-erosion gully on the Tibetan Plateau, Science of The Total
 - Lougheed, V. L., Tweedie, C. E., Andresen, C. G., Armendariz, A. M., Escarzaga, S. M., and Tarin, G.: Patterns and Drivers of Carbon Dioxide Concentrations in Aquatic Ecosystems of the Arctic Coastal Tundra, Global Biogeochemical Cycles, 34, e2020GB006552, https://doi.org/10.1029/2020GB006552, 2020.
- 585 Ma, Q., Jin, H., Yu, C., and Bense, V. F.: Dissolved organic carbon in permafrost regions: A review, Sci. China Earth Sci., 62, 349–364, https://doi.org/10.1007/s11430-018-9309-6, 2019.





- MacDonald, E. N., Tank, S. E., Kokelj, S. V., Froese, D. G., and Hutchins, R. H. S.: Permafrost-derived dissolved organic matter composition varies across permafrost end-members in the western Canadian Arctic, Environ. Res. Lett., 16, 024036, https://doi.org/10.1088/1748-9326/abd971, 2021.
- Manasypov, R. M., Vorobyev, S. N., Loiko, S. V., Kritzkov, I. V., Shirokova, L. S., Shevchenko, V. P., Kirpotin, S. N., Kulizhsky, S. P., Kolesnichenko, L. G., Zemtzov, V. A., Sinkinov, V. V., and Pokrovsky, O. S.: Seasonal dynamics of organic carbon and metals in thermokarst lakes from the discontinuous permafrost zone of western Siberia, Biogeosciences, 12, 3009–3028, https://doi.org/10.5194/bg-12-3009-2015, 2015.
 - Mann, P. J., Sobczak, W. V., LaRue, M. M., Bulygina, E., Davydova, A., Vonk, J. E., Schade, J., Davydov, S., Zimov, N.,
- Holmes, R. M., and Spencer, R. G. M.: Evidence for key enzymatic controls on metabolism of Arctic river organic matter, Global Change Biology, 20, 1089–1100, https://doi.org/10.1111/gcb.12416, 2014.
 - Mann, P. J., Eglinton, T. I., McIntyre, C. P., Zimov, N., Davydova, A., Vonk, J. E., Holmes, R. M., and Spencer, R. G. M.: Utilization of ancient permafrost carbon in headwaters of Arctic fluvial networks, Nat Commun, 6, 7856, https://doi.org/10.1038/ncomms8856, 2015.
- Marschner, B. and Kalbitz, K.: Controls of bioavailability and biodegradability of dissolved organic matter in soils, Geoderma, 113, 211–235, https://doi.org/10.1016/S0016-7061(02)00362-2, 2003.
 - Matveev, A., Laurion, I., and Vincent, W. F.: Winter Accumulation of Methane and its Variable Timing of Release from Thermokarst Lakes in Subarctic Peatlands, Journal of Geophysical Research: Biogeosciences, 124, 3521–3535, https://doi.org/10.1029/2019JG005078, 2019.
- Mazoyer, F., Laurion, I., and Rautio, M.: The dominant role of sunlight in degrading winter dissolved organic matter from a thermokarst lake in a subarctic peatland, Biogeosciences, 19, 3959–3977, https://doi.org/10.5194/bg-19-3959-2022, 2022.
 McCallister, S. L., Ishikawa, N. F., and Kothawala, D. N.: Biogeochemical tools for characterizing organic carbon in inland aquatic ecosystems, Limnology and Oceanography Letters, 3, 444–457, https://doi.org/10.1002/lol2.10097, 2018.
 McDowell, W. H., Zsolnay, A., Aitkenhead-Peterson, J. A., Gregorich, E. G., Jones, D. L., Jödemann, D., Kalbitz, K.,
- Marschner, B., and Schwesig, D.: A comparison of methods to determine the biodegradable dissolved organic carbon from different terrestrial sources, Soil Biology and Biochemistry, 38, 1933–1942, https://doi.org/10.1016/j.soilbio.2005.12.018, 2006.
 - Murphy, K. R., Stedmon, C. A., Graeber, D., and Bro, R.: Fluorescence spectroscopy and multi-way techniques. PARAFAC, Analytical Methods, 5, 6557–6566, https://doi.org/10.1039/C3AY41160E, 2013.
- Murphy, K. R., Stedmon, C. A., Wenig, P., and Bro, R.: OpenFluor– an online spectral library of auto-fluorescence by organic compounds in the environment, Analytical Methods, 6, 658–661, https://doi.org/10.1039/C3AY41935E, 2014.
 Muster, S., Heim, B., Abnizova, A., and Boike, J.: Water Body Distributions Across Scales: A Remote Sensing Based Comparison of Three Arctic Tundra Wetlands, Remote Sensing, 5, 1498–1523, https://doi.org/10.3390/rs5041498, 2013.



645



- Nitze, I., Grosse, G., Jones, B. M., Romanovsky, V. E., and Boike, J.: Remote sensing quantifies widespread abundance of permafrost region disturbances across the Arctic and Subarctic, Nat Commun, 9, 5423, https://doi.org/10.1038/s41467-018-07663-3, 2018.
 - Nusch, E. A.: Comparison of different methods for chlorophyll and phaeopigment determination, Archiv für Hydrobiologie, 14, 14–36, 1980.
 - Ola, A., Fortier, D., Coulombe, S., Comte, J., and Domine, F.: The Distribution of Soil Carbon and Nitrogen Stocks Among
- Dominant Geomorphological Terrain Units in Qarlikturvik Valley, Bylot Island, Arctic Canada, Journal of Geophysical Research: Biogeosciences, 127, e2021JG006750, https://doi.org/10.1029/2021JG006750, 2022.

 Olefeldt, D., Goswami, S., Grosse, G., Hayes, D., Hugelius, G., Kuhry, P., McGuire, A. D., Romanovsky, V. E., Sannel, A. B. K., Schwur, F. a. G., and Turetcky, M. P.: Circumpolar distribution and carbon storage of thermolyaret landscapes. Not
 - B. K., Schuur, E. a. G., and Turetsky, M. R.: Circumpolar distribution and carbon storage of thermokarst landscapes, Nat Commun, 7, 13043, https://doi.org/10.1038/ncomms13043, 2016.
- Pacoureau, T., Mazoyer, F., Maranger, R., Rautio, M., and Laurion, I.: Shifts in dissolved organic matter and nutrients in tundra ponds along a gradient of permafrost erosion, Arctic Science, 11, 1–17, https://doi.org/10.1139/as-2024-0060, 2025. Pinheiro, J. and Bates, D.: _nlme: Linear and Nonlinear Mixed Effects Models_, 2023.
 - Pokrovsky, O. S., Karlsson, J., and Giesler, R.: Freeze-thaw cycles of Arctic thaw ponds remove colloidal metals and generate low-molecular-weight organic matter, Biogeochemistry, 137, 321–336, https://doi.org/10.1007/s10533-018-0421-6, 2018.
- Prèskienis, V.: La forte variabilité des émissions de gaz à effet de serre des lacs et des mares de l'Arctique expliquée par la morphologie des plans d'eau, l'activité érosive et la qualité de la matière organique des sols environnants./The high varia bility of greenhouse gas emissions from Arctic lakes and ponds explained by the morphology of water bodies, the erosional activity and the quality of organic matter in surrounding soils., phd, Institut National de la Recherche Scientifique, Québec, 186 pp., 2022.
- Prėskienis, V., Laurion, I., Bouchard, F., Douglas, P. M. J., Billett, M. F., Fortier, D., and Xu, X.: Seasonal patterns in greenhouse gas emissions from lakes and ponds in a High Arctic polygonal landscape, Limnology and Oceanography, 66, S117–S141, https://doi.org/10.1002/lno.11660, 2021.
 - Prėskienis, V., Fortier, D., Douglas, P. M. J., Rautio, M., and Laurion, I.: Permafrost degradation and soil erosion as drivers of greenhouse gas emissions from tundra ponds, Environ. Res. Lett., 19, 014072, https://doi.org/10.1088/1748-9326/ad1433, 2024.
- R Core Team: _R: A Language and Environment for Statistical Computing_. R Foundation for Statistical Computing, 2024. Rodríguez, P., Ask, J., Hein, C. L., Jansson, M., and Karlsson, J.: Benthic organic carbon release stimulates bacterioplankton production in a clear-water subarctic lake, Freshwater Science, 32, 176–182, https://doi.org/10.1899/12-005.1, 2013. Roiha, T., Laurion, I., and Rautio, M.: Carbon dynamics in highly heterotrophic subarctic thaw ponds, Biogeosciences, 12,
- 650 7223–7237, https://doi.org/10.5194/bg-12-7223-2015, 2015.





- Shirokova, L. S., Chupakov, A. V., Zabelina, S. A., Neverova, N. V., Payandi-Rolland, D., Causserand, C., Karlsson, J., and Pokrovsky, O. S.: Humic surface waters of frozen peat bogs (permafrost zone) are highly resistant to bio- and photodegradation, Biogeosciences, 16, 2511–2526, https://doi.org/10.5194/bg-16-2511-2019, 2019.
- Smith, E. M. and Prairie, Y. T.: Bacterial metabolism and growth efficiency in lakes: The importance of phosphorus availability, Limnology and Oceanography, 49, 137–147, https://doi.org/10.4319/lo.2004.49.1.0137, 2004.
 - Spencer, R. G. M., Mann, P. J., Dittmar, T., Eglinton, T. I., McIntyre, C., Holmes, R. M., Zimov, N., and Stubbins, A.: Detecting the signature of permafrost thaw in Arctic rivers, Geophysical Research Letters, 42, 2830–2835, https://doi.org/10.1002/2015GL063498, 2015.
- Stubbins, A., Lapierre, J.-F., Berggren, M., Prairie, Y. T., Dittmar, T., and del Giorgio, P. A.: What's in an EEM? Molecular Signatures Associated with Dissolved Organic Fluorescence in Boreal Canada, Environ. Sci. Technol., 48, 10598–10606, https://doi.org/10.1021/es502086e, 2014.
 - Tank, S. E., Vonk, J. E., Walvoord, M. A., McClelland, J. W., Laurion, I., and Abbott, B. W.: Landscape matters: Predicting the biogeochemical effects of permafrost thaw on aquatic networks with a state factor approach, Permafrost and Periglacial Processes, 31, 358–370, https://doi.org/10.1002/ppp.2057, 2020.
- Vähätalo, A. V. and Wetzel, R. G.: Long-term photochemical and microbial decomposition of wetland-derived dissolved organic matter with alteration of 13C:12C mass ratio, Limnology and Oceanography, 53, 1387–1392, https://doi.org/10.4319/lo.2008.53.4.1387, 2008.
 - Vidal, L. O., Granéli, W., Daniel, C. B., Heiberg, L., and Roland, F.: Carbon and phosphorus regulating bacterial metabolism in oligotrophic boreal lakes, Journal of Plankton Research, 33, 1747–1756, https://doi.org/10.1093/plankt/fbr059, 2011.
- Vonk, J. E., Mann, P. J., Davydov, S., Davydova, A., Spencer, R. G. M., Schade, J., Sobczak, W. V., Zimov, N., Zimov, S., Bulygina, E., Eglinton, T. I., and Holmes, R. M.: High biolability of ancient permafrost carbon upon thaw, Geophysical Research Letters, 40, 2689–2693, https://doi.org/10.1002/grl.50348, 2013.
 - Vonk, J. E., Tank, S. E., Mann, P. J., Spencer, R. G. M., Treat, C. C., Striegl, R. G., Abbott, B. W., and Wickland, K. P.: Biodegradability of dissolved organic carbon in permafrost soils and aquatic systems: a meta-analysis, Biogeosciences, 12,
- 675 6915–6930, https://doi.org/10.5194/bg-12-6915-2015, 2015a.
 - Vonk, J. E., Tank, S. E., Bowden, W. B., Laurion, I., Vincent, W. F., Alekseychik, P., Amyot, M., Billet, M. F., Canário, J., Cory, R. M., Deshpande, B. N., Helbig, M., Jammet, M., Karlsson, J., Larouche, J., MacMillan, G., Rautio, M., Walter Anthony, K. M., and Wickland, K. P.: Reviews and syntheses: Effects of permafrost thaw on Arctic aquatic ecosystems, Biogeosciences, 12, 7129–7167, https://doi.org/10.5194/bg-12-7129-2015, 2015b.
- Vonk, J. E., Tank, S. E., and Walvoord, M. A.: Integrating hydrology and biogeochemistry across frozen landscapes, Nat Commun, 10, 5377, https://doi.org/10.1038/s41467-019-13361-5, 2019.
 - von Wachenfeldt, E. and Tranvik, L. J.: Sedimentation in Boreal Lakes—The Role of Flocculation of Allochthonous Dissolved Organic Matter in the Water Column, Ecosystems, 11, 803–814, https://doi.org/10.1007/s10021-008-9162-z, 2008.





- Ward, C. P., Nalven, S. G., Crump, B. C., Kling, G. W., and Cory, R. M.: Photochemical alteration of organic carbon draining permafrost soils shifts microbial metabolic pathways and stimulates respiration, Nat Commun, 8, 772, https://doi.org/10.1038/s41467-017-00759-2, 2017.
 - Weishaar, J. L., Aiken, G. R., Bergamaschi, B. A., Fram, M. S., Fujii, R., and Mopper, K.: Evaluation of Specific Ultraviolet Absorbance as an Indicator of the Chemical Composition and Reactivity of Dissolved Organic Carbon, Environ. Sci. Technol., 37, 4702–4708, https://doi.org/10.1021/es030360x, 2003.
- Wetzel, R. G., Hatcher, P. G., and Bianchi, T. S.: Natural photolysis by ultraviolet irradiance of recalcitrant dissolved organic matter to simple substrates for rapid bacterial metabolism, Limnology and Oceanography, 40, 1369–1380, https://doi.org/10.4319/lo.1995.40.8.1369, 1995.
 - Wologo, E., Shakil, S., Zolkos, S., Textor, S., Ewing, S., Klassen, J., Spencer, R. G. M., Podgorski, D. C., Tank, S. E., Baker, M. A., O'Donnell, J. A., Wickland, K. P., Foks, S. S. W., Zarnetske, J. P., Lee-Cullin, J., Liu, F., Yang, Y., Kortelainen, P.,
- Kolehmainen, J., Dean, J. F., Vonk, J. E., Holmes, R. M., Pinay, G., Powell, M. M., Howe, J., Frei, R. J., Bratsman, S. P., and Abbott, B. W.: Stream Dissolved Organic Matter in Permafrost Regions Shows Surprising Compositional Similarities but Negative Priming and Nutrient Effects, Global Biogeochemical Cycles, 35, e2020GB006719, https://doi.org/10.1029/2020GB006719, 2021.
- Wyatt, K. H. and Rober, A. R.: Warming enhances the stimulatory effect of algal exudates on dissolved organic carbon decomposition, Freshwater Biology, 65, 1288–1297, https://doi.org/10.1111/fwb.13390, 2020.
 - Zhang, X., Hutchings, J. A., Bianchi, T. S., Liu, Y., Arellano, A. R., and Schuur, E. A. G.: Importance of lateral flux and its percolation depth on organic carbon export in Arctic tundra soil: Implications from a soil leaching experiment, Journal of Geophysical Research: Biogeosciences, 122, 796–810, https://doi.org/10.1002/2016JG003754, 2017.